When can we expect extremely high surface temperatures?

Andreas Sterl,[1] Camiel Severijns,[1] Henk Dijkstra,[2] Wilco Hazeleger,[1] Geert Jan van Oldenborgh,[1] Michiel van den Broeke,[2] Gerrit Burgers,[1] Bart van den Hurk,[1,2] Peter Jan van Leeuwen,[2] Peter van Velthoven[1]

Andreas Sterl (sterl@knmi.nl), Camiel Severijns, Wilco Hazeleger, Gerrit Burgers, Bart van den Hurk, Geert Jan van Oldenborgh, Peter van Velthoven, Royal Netherlands Institute of Meteorology (KNMI), P.O. Box 201, NL-3730 AE De Bilt, The Netherlands; Henk Dijkstra, Peter Jan van Leeuwen, Michiel van den Broeke, Institute for Marine and Atmospheric Research Utrecht (IMAU), Utrecht University, P.O. Box 80005, NL-3508 TA Utrecht, The Netherlands

[1]Royal Netherlands Meteorological Institute (KNMI), De Bilt, Netherlands

[2]Institute for Marine and Atmospheric Research Utrecht (IMAU), Utrecht University, Utrecht, Netherlands

In the Essence project a 17-member ensemble simulation of climate change in response to the SRES A1b scenario has been carried out using the ECHAM5/MPI-OM climate model. The relatively large size of the ensemble makes it possible to accurately investigate changes in extreme values of climate variables. Here we focus on the annual-maximum 2m-temperature and fit a Generalized Extreme Value (GEV) distribution to the simulated values and investigate the development of the parameters of this distribution. Over most land areas both the location and the scale parameter increase. Consequently the 100-year return values increase faster than the average temperatures. A comparison of simulated 100-year return values for the present climate with observations (station data and reanalysis) shows that the ECHAM5/MPI-OM model, as well as other models, overestimates extreme temperature values. After correcting for this bias, it still shows values in excess of 50°C in Australia, India, the Middle East, North Africa, the Sahel and equatorial and subtropical South America at the end of the century.

1. Introduction

An important issue in climate research is to assess and predict the changes in extreme events in a future warmer climate [*IPCC*, 2007]. Many urgent questions raised by policy makers are concerned with changes in the probability of extreme events, such as extremely hot summers and heavy rainfall, over the next decades. For example, very high temperatures can be fatal [*Patz et al.*, 2005] and are therefore much more important than average temperatures when assessing the consequences of climate change.

Changes in temperature extremes tend to follow mean temperature changes in many parts of the world [*Kharin and Zwiers*, 2005]. Analyses of 20-year return values of annual extremes of near-surface temperatures from the coupled ocean-atmosphere general circulation models (CGCMs) used in the IPCC AR4 indicate that cold extremes warm faster than warm extremes by about 30% – 40% globally averaged [*Kharin et al.*, 2007]. *Lobell et al.* [2007] analyzed changes in mean daily maximum temperatures and their relation with cloud cover using the same AR4 model results. They find that inter-model standard deviations of June-August mean daily maximum temperatures are more than 50% larger than for the mean daily minimum temperatures, pointing to large model uncertainties. *Clark et al.* [2006] used a perturbed physics ensemble of the Third Hadley Centre Atmospheric Model (HadAM3) to assess changes in daily maximum and minimum temperatures. Their results also indicate that cold extremes warm faster than warm extremes, and that warm extremes warm faster than average temperatures.

In this paper we focus on extremely high temperatures, represented by the 100-year return temperature. Motivation for this study is that Western Europe has experienced

two very rare hot summers in 2003 and 2006. Based on available observations, which sometimes date back to early 1700, the return times associated with the temperatures in these years reached several thousand years [*Schär et al.*, 2004]. One can use Extreme Value Theory (EVT) to determine 100-year return values and changes in these values using AR4 model output. For instance *Parey* [2008] applied this approach to regional model output from the PRUDENCE project to compute 100-year return values of temperature for France.

With more ensemble members for a particular model configuration, uncertainties in estimates of parameters in EVT will decrease. The usefulness of a large ensemble of simulations was demonstrated by *Selten et al.* [2003]. In the Essence project a suite of ensemble climate simulations has been performed using one of the AR4 models, the ECHAM5/MPI-OM (see below). In the present study we focus on the changes in T_{100}, the annual-maximum 2m-temperature that on average occurs once in 100 years, under the IPCC SRES A1b scenario [*Nakicenovic et al.*, 2000]. Due to the large ensemble the possible range of the annual-maximum 2m-temperature is well-sampled and a reliable picture of T_{100} and its future development can be gained using EVT. Furthermore, we use the model bias with respect to the observations to produce bias corrected T_{100} for the end of this century.

2. Model and experiments

2.1. Model

The ECHAM5/ MPI-OM is a coupled climate model which has been developed at the Max-Planck-Institute for Meteorology in Hamburg. The model was chosen because it

performed well on a number of criteria during an intercomparison of all AR4 models, such as the atmospheric circulation over Europe and the Tropical Pacific climate [*Van Ulden and Van Oldenborgh*, 2006]. The two component models, ECHAM5 for the atmosphere and MPI-OM for the ocean, are well documented (ECHAM5: *Roeckner et al.* [2003], MPI-OM: *Marsland et al.* [2003]), and a Special Section of the *Journal of Climate* was devoted to the coupled model and its validation (vol. 19(16), pp 3769-3987). The version used here is the same that has been used for climate scenario runs in preparation of AR4. ECHAM5 is run at a horizontal resolution of T63 and 31 vertical hybrid levels with the top level at 10 hPa. The ocean model MPI-OM is a primitive equation z-coordinate model with a variable horizontal resolution.

2.2. Numerical Experiments

The baseline simulation period is 1950-2100. For the historical part (1950-2000) the concentrations of greenhouse gases (GHG) and tropospheric sulfate aerosols are specified from observations, while for the future part (2001-2100) they follow the SRES A1b scenario [*Nakicenovic et al.*, 2000]. Stratospheric aerosols from volcanic eruptions are not taken into account, and the solar constant is fixed. The runs are initialized from a long run in which historical GHG concentrations have been used until 1950. Different ensemble members are generated by disturbing the initial state of the atmosphere. Gaussian noise with an amplitude of 0.1 K is added to the initial temperature field. The initial ocean state is not perturbed.

The standard ensemble consists of 17 runs driven by a time-varying forcing as described above. Model parameters are as described by *Roeckner et al.* [2003] (ECHAM5) and

Marsland et al. [2003] (MPI-OM). Additionally, three experimental ensembles have been performed to study the impact of some key parameterizations, again making use of the ensemble strategy to increase the signal-to-noise ratio. While most 3-dimensional fields are stored as monthly means, some atmospheric fields are also available as daily means. Some surface fields like temperature and wind speed are available at a time resolution of 3 hours. This makes a thorough analysis of weather extremes and their possible variation in a changing climate possible. The data are stored at the full model resolution (see www.knmi.nl/∼sterl/Essence).

The projected global-mean temperature increases by 3.5 K between 2000 and 2100, which is at the upper end of the range given by the models analyzed in the IPCC AR4 (see [*IPCC*, 2007], Fig. 10.5). Up to 2007, the increase is within error margins equal to the observed trend with a ratio of 1.06 ± 0.06 with the HadCRUT3 estimate of global mean temperature anomalies [*Brohan et al.*, 2006], giving confidence in the model's sensitivity to GHG concentrations. Over most areas the modeled trends in local temperature are also within the error margins of the observed trends.

3. Results

To determine the statistics of extremely high temperatures and its development in time we divide the results from the 17 standard ensemble simulations into slices of 10 years (1950-1959, 1960-1969, etc) and fit the resulting 170 annual maxima of T_{2m} in each slice to a Generalized Extreme Value (GEV) distribution, the theoretical distribution for block maxima (Coles 2001),

$$G(x) = \exp\{-[1 + \xi\,(\frac{x-\mu}{\sigma})]^{-1/\xi}\}. \quad (1)$$

Here μ, σ and ξ are called the location, scale and shape parameter, respectively. $G(x)$ is defined for $\{x : 1+\xi\,(\frac{x-\mu}{\sigma}) > 0\}$, so that for negative ξ the distribution has a hard upper bound of $\mu - \sigma/\xi$. The return time $T(x)$ for level x is given by the $1 - 1/T(x)$ percentile of G, i.e.,

$$T(x) = \frac{1}{1 - G(x)}. \tag{2}$$

Due to the large number of samples per time-slice (170) the resulting estimates of the distribution parameters have small error bars. This is shown in Figure 1, where the temperature is plotted versus the return time for a location in southern France for different decades together with the 95% confidence intervals as obtained from a bootstrap calculation (1000 samples). The GEV provides a good fit to the data. The spread of the actual values (black crosses) around the fit line is small, and the calculated uncertainty for T_{100} is less than 2 K. These characteristics are also found at other locations. *Kharin et al.* [2007] show that the inter-model spread for the 20-year return temperatures already amounts to several Kelvin. Therefore, the sampling error in the Essence results is much lower than the model error.

Figure 1 also shows that future temperature extremes are governed by the same processes as today's extremes. If new processes were to come in, they would show up as deviations from the fit at the highest simulated temperatures. That we do not see any such deviation implies that the processes leading to future extreme temperatures are already at work now. They simply become more frequent, increasing their impact. This finding is also typical for other locations.

Over the period 1958-2001, we compared the modeled T_{100}-values with values derived from the ERA-40 reanalysis [*Uppala et al.*, 2004], which also outputs maximum temperature, and with the gridded HadGHCND dataset [*Caesar et al.*, 2006] of observed daily maximum temperatures. The T_{100} values from ERA-40 agree well with those derived from the HadGHCND gridded data (not shown).

Figure 1 shows that at the given location Essence overestimates T_{100} for the present climate with respect to values derived from ERA-40. Figure 2 shows that this is a general property of the model. Modeled return values are up to 10 K higher than values derived from the reanalysis, and the overestimation is largest in dry areas (Mediterranean, Middle East, South Africa, Australia), while the maxima are underestimated in Siberia. The biases in extreme and in mean temperatures have similar pattern and amplitude (not shown). T_{100} is underestimated over sea (Figure 2) because SST in Essence is lower than in ERA-40. Variability is low, and T_{100} is determined by the mean temperature.

The difference pattern in Figure 2 is quite similar to that obtained by *Kharin et al.* [2007] (their Figure 4) for the 20-year return values from 16 AR4-models. Thus the overestimation of extreme temperatures is not an artifact of the ECHAM5/MPI-OM model, but a general deficiency of the present generation of climate models. Also *Parey* [2008] notes that only a few of the investigated regional climate models are able to correctly reproduce observed extreme temperatures. Therefore caution is needed when interpreting projected T_{100}-values. The same model deficiencies that cause an overestimation of present-day extreme temperatures (e.g., in the Middle East) may become effective in areas

where present-day extremes are well represented and lead to an overestimation of future values.

The increase in T_{100} is displayed in Figure 3a as a multiple of the ensemble mean temperature change. The largest simulated increase occurs in regions where the soil is drying out. It seems therefore plausible that models have difficulties to simulate very dry conditions. As was already noted in earlier work [*Kharin et al.*, 2007], the extremes rise faster than the means in a warming climate. The increase is brought about by increases in both the location parameter μ and the scale parameter σ (not shown). The first reflects the fact that the climate becomes warmer, the second that it becomes more variable (cf. Eq. (1)). The change in μ is positive everywhere and larger over land than over sea. The largest changes are found over southern Europe and northern South America, followed by South Africa and the Middle East. The change of the scale parameter σ has a different pattern. It is positive over most land areas with maxima over Europe and parts over North America. These patterns correspond well with those found by *Clark et al.* [2006] (their Fig.$\tilde{4}$). The shape parameter ξ shows no systematic changes and remains negative (not shown). Where both μ and σ increase, the change of T_{100} is largest. This is the case over Europe and an area south of the Great Lakes in North America (Figure 3a).

Figure 3b shows T_{100} for the period 2090-2100, corrected for the bias in present-day values (i.e., Fig. 2 is subtracted). According to this figure, temperature extremes reach values around 50°C in large parts of the area equatorward of 30°. This includes heavily populated areas like India and the Middle East. In much of the US, in southern Europe and in the populated regions of Australia values far exceeding 40°C are reached. Such

temperatures, if lasting for some days, are life threatening and receive relatively little attention in the climate change debate.

Figure 3b shows the development of bias-corrected T_{100} at a few 'hot spots' from Figure 3b. It is seen that the increase in northern India is quite regular, reaching 48°C in the middle of the century and 50°C near the end. In this region the shift of the temperature distribution due to global warming is the main cause of change. In contrast, in equatorial South America and the American Mid-West, the increase is faster and more erratic. Here, the increase in variability accelerates the temperature rise in hot extremes, which reach 48°C in the Midwest and 54°C in South America in 2100. The European points show a slightly less accelerated increase, but around 2050 (2100) T_{100} is modeled to be 4 (7) K warmer than in the present-day climate.

4. Discussion and Conclusion

In the Essence project a 17-member ensemble of future climate development using a state-of-the-art climate model (ECHAM5/MPI-OM) has been performed giving a global mean surface warming of 3.5 K by the end of this century under the SRES A1b scenario. Using the data from this ensemble, we have determined the changes in parameters in the GEV distribution of extreme annual maximum temperatures and in particular the changes in T_{100} values. The latter increase faster than the global mean temperature. We find no second population in the extreme value analysis, which would show up as deviations from the GEV fit for large return times, and as changes in the parameter ξ in (1). This suggests that in this model the processes that determine more moderate extremes, e.g., T_{20} values [*Kharin et al.*, 2007], are also responsible for high extreme values.

The main results of this paper are in agreement with those of *Clark et al.* [2006], indicating that the patterns of modeled changes of extreme temperatures are not an artifact of the particular model used here. Even if corrected for the bias in today's climate, the projected T_{100} values point to the importance of dangerously high future temperatures in densely populated areas. For example, projected T_{100} values far exceed 40°C in Southern Europe, the US Mid-West by 2090-2100 and even reach 50°C in north-eastern India and most of Australia. Such levels receive much too little attention in the current climate change discussion, given the potentially large implications.

There are worryingly large biases in the simulation of present-day extremes, which imply that the modeled future values may be biased. To improve estimates of the probability of extremely high temperatures in the coming decades, good observational data sets and investigations into the reasons for model biases affecting extreme temperatures are needed. However, even with these uncertainties, a 10% chance of exceeding 48°C every decade at any point in the red regions of Fig. 3b is a risk that should be taken seriously.

Acknowledgments. ESSENCE is a DEISA-DECI project and was carried out with support of DEISA (Distributed European Infrastructure for Supercomputing Applications, www.deisa.org), HLRS (High Performance Computing Center Stuttgart, www.hlrs.de), SARA (Dutch High Performance Computing Center, www.sara.nl) and NCF (Netherlands National Computing Facilities foundation) through NCF projects NRG-2006.06, CAVE-06-023 and SG-06-267). We thank HLRS and SARA staff, especially Wim Rijks and Jorrit Adriaanse, for their excellent technical support. The Max-Planck-Institute for Meteorology in Hamburg (www.mpimet.mpg.de) made available their

climate model ECHAM5/MPI-OM and provided valuable advice on implementation and use of the model. We are especially indebted to Monika Esch and Helmuth Haak.

References

Brohan, P., J.J. Kennedy, I. Harris, S.F.B. Tett and P.D. Jones (2006), Uncertainty estimates in regional and global observed temperature changes: a new dataset from 1850, *J. Geophys. Res. 111*, D12106, doi:10.1029/2005JD006548.

Caesar, J., and L. Alexander (2006), Large-scale changes in observed daily maximum and minimum temperatures: Creation and analysis of a new gridded data set, *J. Geophys. Res. 111*, D05101, doi:10.1029/2005JD006280.

Clark, R.T., S.J. Brown, and J.M. Murphy (2006), Modeling Northern Hemisphere summer heat extreme changes and their uncertainties using a physics ensemble of climate sensitivity experiments, *J. Clim. 19*, 4418-4435.

Coles, S. (2001), *An Introduction to Statistical Modeling of Extreme Values*, 208 pp, Springer-Verlag, Berlin, London, Heidelberg.

IPCC (2007): Climate Change 2007, The Physical Science Basis. *Contribution of Working Group I to the Fourth Assessment Report on the Intergovernmental Panel on Climate Change*, [Solomon, S., D. Qin, M. Manning, Z. Chen, M. Marquis, K.B. Averyt, M. Tignor and H.L. Miller (eds.)] Cambridge University Press, Cambridge, United Kingdom and New York, USA, 996 pp.

Kharin, V.V., and F.W. Zwiers (2005), Estimating extremes in transient climate change simulations, *J. Clim.*, *18*, 1156-1173.

Kharin, V.V., F.W. Zwiers, X. Zhang, and G.C. Hegerl (2007), Changes in temperature and precipitation extremes in the IPCC ensemble of global coupled model simulations, *J. Clim.*, *20*, 1419-1444, doi: 10.1175/JCLI4066.1.

Lobell, D.B., C. Bonfils, and P.B. Duffy (2007), Climate change uncertainty for daily minimum and maximum temperatures: A model inter-comparison, *Geophys. Res. Lett.*, *34*, L05715, doi: 10.1029/2006GL028726.

Marsland, S.J., H. Haak, J.H. Jungclaus, M. Latif, and F. Röske (2003), The Max-Planck-Institute global ocean/sea ice model with orthogonal curvilinear coordinates, *Ocean Modelling 5*, 91-127.

Nakicenovic, N. et al. (2000), *Special Report on Emissions Scenarios: A Special Report of Working Group III of the Intergovernmental Panel on Climate Change*, 599 pp., Cambridge University Press, Cambridge, U.K. Available online at: www.grida.no/climate/ipcc/emission/index.htm.

Parey, S. (2008), Extremely high temperatures in France at the end of the century, *Clim. Dyn.*, *30*, 99-112, doi: 10.1007/s00382-007-0275-4.

Patz, J.A., D. Campbell-Lendrum, T. Holloway, and J.A. Foley (2005), Impact of regional climate change on human health, *Nature*, *438*, 310-317, doi: 10.1038/nature04188.

Roeckner, E., G. Bäuml, L. Bonaventura, R. Brokopf, M. Esch, M. Giorgetta, S. Hagemann, I. Kirchner, L. Kornblueh, E. Manzini, A. Rhodin, U. Schlese, U. Schulzweida, and A. Tompkins (2003), The atmospheric general circulation model ECHAM 5. PART I: Model description, *Report No. 349*, Max-Planck-Institut für Meteorologie, Hamburg, Germany, 127 pages.

Schär, C., P.L. Vidale, D. Lüthi, C. Frei, C. Häberli, M.A. Linger, and C. Appenzeller (2004), The role of increasing temperature variability in European summer heatwaves, *Nature*, *427*, 332-336.

Selten, F.M., G.W. Branstator, H.A. Dijkstra, and M. Kliphuis (2004), Tropical origins for recent and future Northern Hemisphere climate change, *Geophys. Res. Lett.*, *31*, L21205, doi: 10.1029/2004GL020739.

Uppala, S., and 44 co-authors (2005), The ERA-40 re-analysis, *Quart. J. Roy. Meteor. Soc.*, *131*, 2961-3012, doi: 10.1256/qj.04.176.

Van Ulden, A.P., and G.J. van Oldenborgh (2006), Large-scale atmospheric circulation biases and changes in global climate model simulations and their importance for regional climate scenarios: a case study for West-Central Europe, *Atmos. Chem. Phys.*, *6*, 863-881, SRef-ID: 1680-7324/acp/2006-6-863.

Figure 1. *GEV-fit for annual-maximum T_{2m} at a location in Southern France (2°E, 42°N) as a function of return time (see (2)) for different time slices, together with the values derived from ERA-40 for the period 1958-2002. The colored lines are the fits to the actual annual-maximum values that are represented by the black dots. The colored crosses indicate the respective 95%-confidence interval, based on a bootstrap with 1,000 repetitions.*

Figure 2. *T_{100} from Essence (whole ensemble) minus T_{100} from ERA-40 for the entire ERA-40 period (1958-2001).*

Figure 3. *(a) Difference between 2090-2099 and 1990-1999 of T_{100}, expressed as a multiple of the ensemble mean temperature change during the same period. Red (blue) colors mean that T_{100} grows faster (slower) than the mean temperature. (b) T_{100} from Essence for the period 2090-2100, corrected for the bias with respect to ERA-40 (see Fig. 2). (c) Time series of T_{100} at selected places, bias corrected using ERA-40. The years denote the middle of the respective time-slice of ten years.*

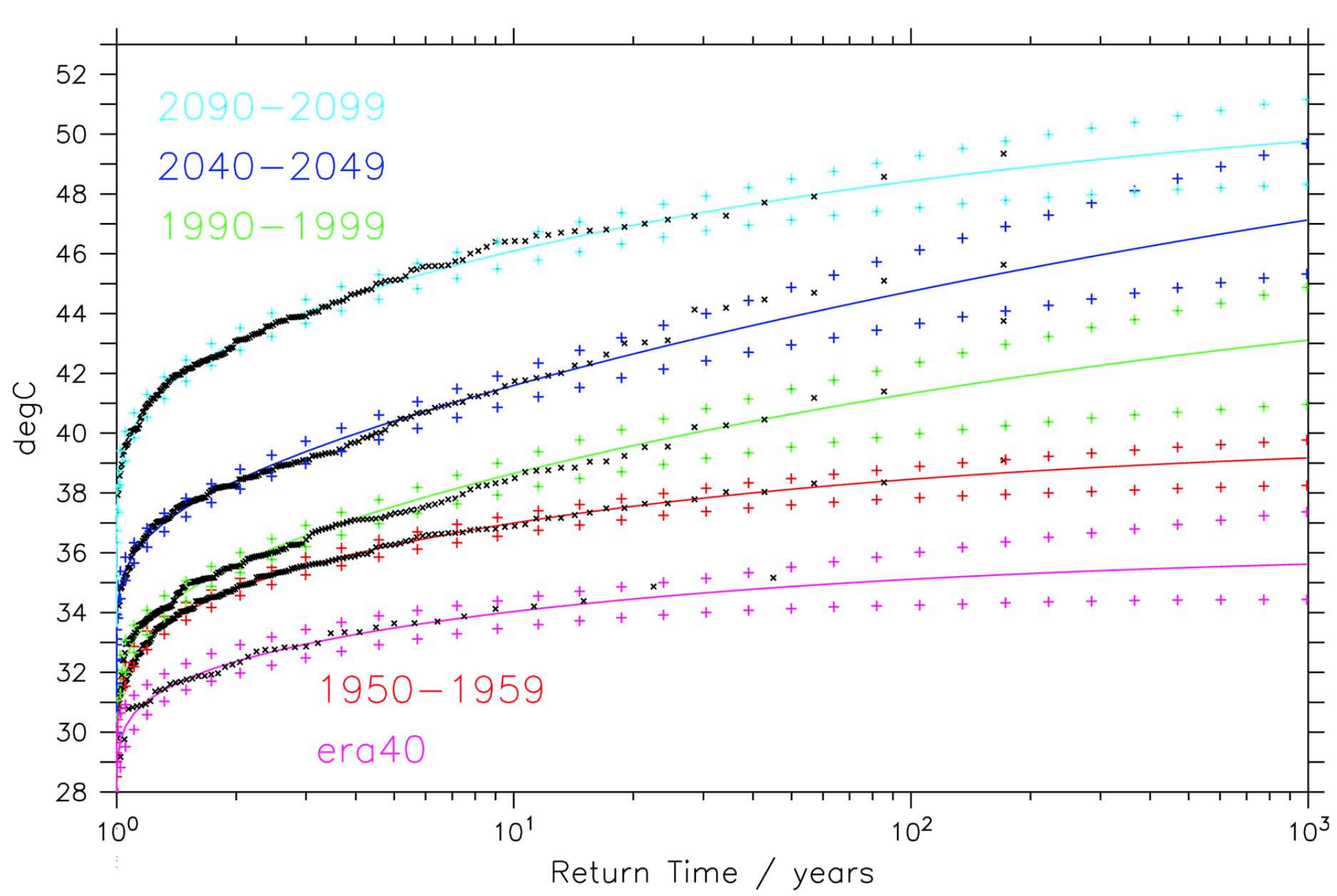
2090–2099
2040–2049
1990–1999
1950–1959
era40
degC
Return Time / years
52
50
48
46
44
42
40
38
36
34
32
30
28
10^0
10^1
10^2
10^3

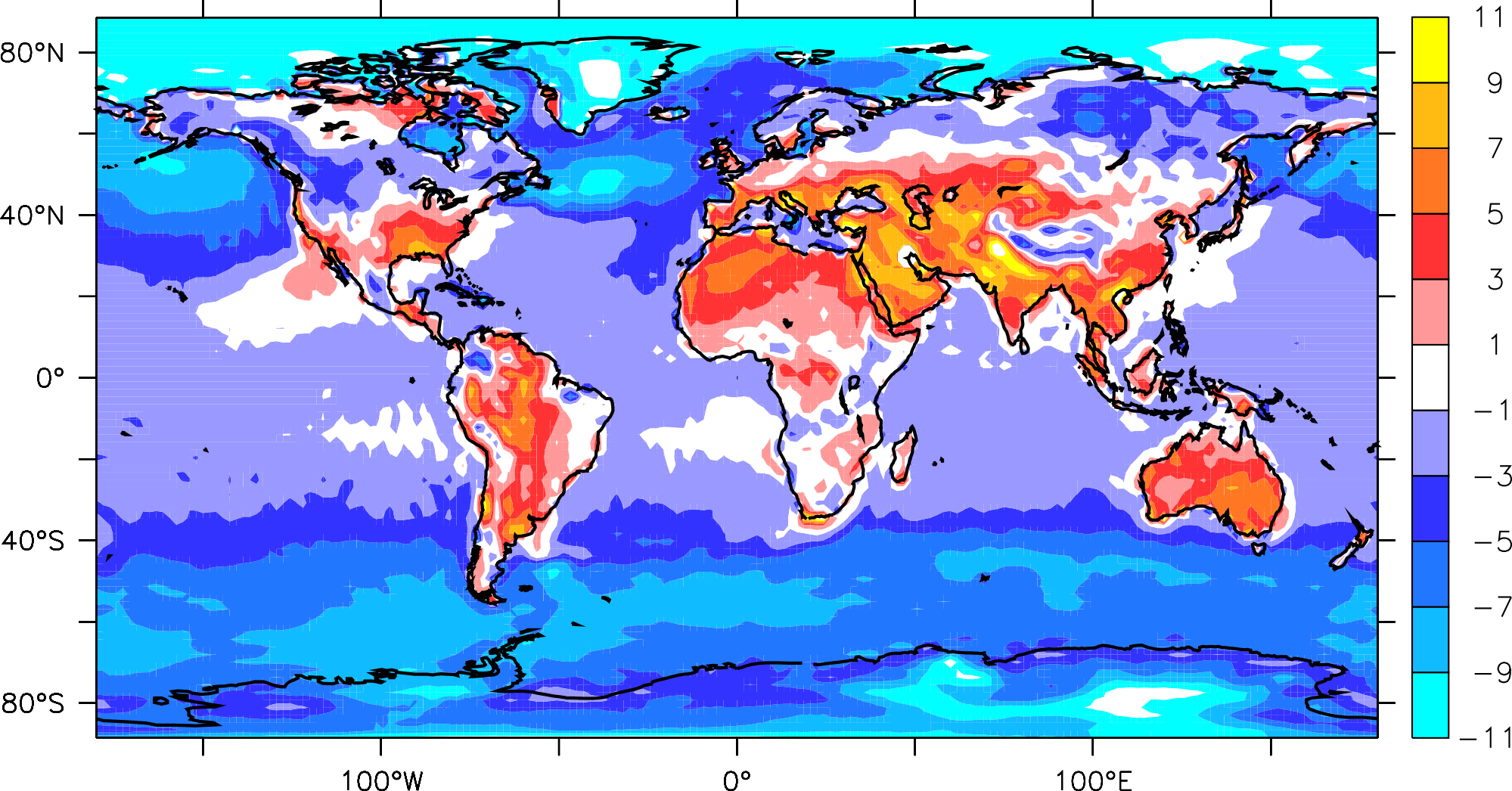
80°N
40°N
0°
40°S
80°S
100°W
0°
100°E
11
9
7
5
3
1
−1
−3
−5
−7
−9
−11

a) ΔT_{100}

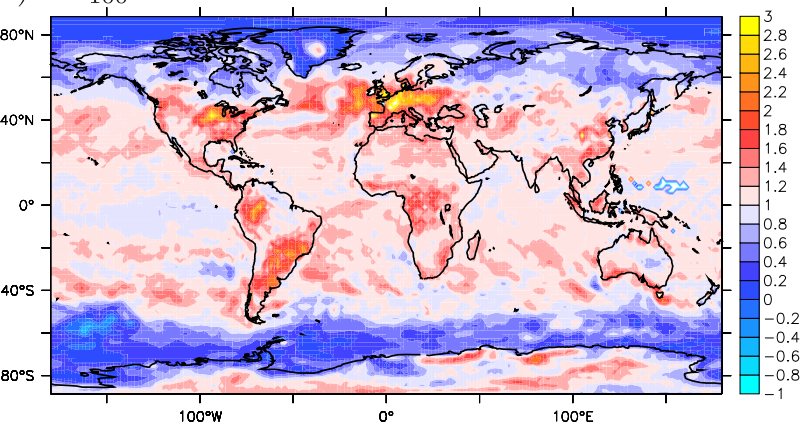

b) T_{100} Essence, bias-corrected

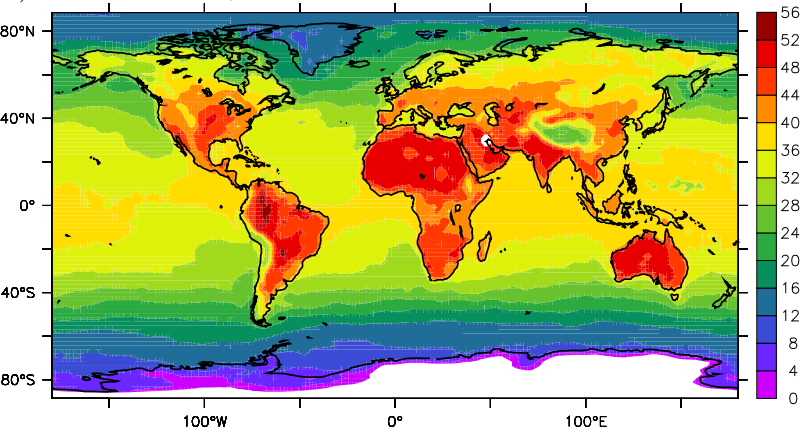

c) Example times series